Published in final edited form as:

Invest Radiol. 2018 February ; 53(2): 87–95. doi:10.1097/RLI.0000000000000414.

Quantitative proton spectroscopy of the testes at 3 tesla: towards a noninvasive biomarker of spermatogenesis

Pippa Storey, PhD[1], **Oded Gonen, PhD**[1], **Andrew B. Rosenkrantz, MD**[1], **Kiranpreet K. Khurana, MD**[2,3], **Tiejun Zhao, PhD**[4], **Rajesh Bhatta, RT**[1], and **Joseph P. Alukal, MD**[2]

[1]Radiology Department, New York University School of Medicine, New York, NY, United States

[2]Urology Department, New York University School of Medicine, New York, NY, United States

[3]Urology Department, Case Western Reserve University, Cleveland, OH, United States

[4]Siemens Healthcare, New York, NY, United States

Abstract

Objectives—To compare testicular metabolite concentrations between fertile control subjects and infertile men.

Materials and Methods—Single voxel ^{1}H-MRS was performed in the testes with and without water suppression at 3T in 9 fertile control subjects and 9 infertile patients (8 with azoospermia and 1 with oligospermia). In controls only, the T1 and T2 values of water and metabolites were also measured. Absolute metabolite concentrations were calculated using the unsuppressed water signal as a reference and correcting for the relative T1 and T2 weighting of the water and metabolite signals.

Results—Testicular T1 values of water, total choline and total creatine were 2028 ± 125 ms, 1164 ± 105 ms and 1421 ± 314 ms respectively (mean ± standard deviation). T2 values were 154 ± 11 ms, 342 ± 53 ms and 285 ± 167 ms respectively. Total choline concentration was lower in patients (mean 1.5mM, range 0.9 – 2.1mM) than controls (mean 4.4mM, range 3.2 – 5.7mM), $p = 4 \times 10^{-5}$. Total creatine concentration was likewise reduced in patients (mean 1.1mM, range: undetectable – 2.7mM) compared to controls (mean 3.6mM, range 2.5 – 4.7mM), $p = 1.6 \times 10^{-4}$. The myo-inositol signal normalized to the water reference was also lower in patients than controls ($p = 4 \times 10^{-5}$).

Conclusions—Testicular metabolite concentrations, measured by proton spectroscopy at 3T, may be valuable as noninvasive biomarkers of spermatogenesis.

Keywords

^{1}H-MRS; testis; spermatogenesis; male infertility; azoospermia; micro-TESE; choline; creatine; myo-inositol

Corresponding author: Pippa Storey, Center for Biomedical Imaging, 660 First Avenue, 4th Floor, New York, NY 10016, Tel: 212-263 4854, Fax: 212-263 7541, pippa.storey@nyumc.org.

Conflicts of Interest

The authors report no conflict of interest.

Introduction

Approximately 1% of all men and 10 – 15% of infertile men are azoospermic (i.e. they have no sperm in their semen) [1]. In most cases of azoospermia, no obstruction can be identified in the reproductive tract, and the condition is attributed to impaired or incomplete spermatogenesis. Some men with non-obstructive azoospermia (NOA) may nevertheless have small numbers of sperm in their testes. These can be harvested by removing tissue from the testis and opening the seminiferous tubules under stereomicroscopy. Sperm extracted in this manner can then be used to achieve fertilization via intracytoplasmic sperm injection (ICSI), in which a single spermatozoon is injected directly into a mature egg. ICSI is performed as an adjunct to in vitro fertilization (IVF) and allows conceptions even with minimal sperm recovery.

Methods of sperm retrieval have evolved considerably over the years, with concomitant increases in success rates and reductions in morbidity [2]. The current state of the art is microdissection testicular sperm extraction (micro-TESE) [3], a procedure performed under general anesthesia in which the tunica albuginea is opened widely and seminiferous tubules are removed under a high-power operative microscope, allowing the surgeon to avoid blood vessels and target tubules that are most likely to contain sperm based on their size and opacity. However, in 40 – 60% of patients undergoing micro-TESE, no sperm are found [4–6]. These men could have been spared the risks [4–6] and expense of surgery if a noninvasive technique were available to determine the presence or absence of sperm in advance. Furthermore, because micro-TESE is often scheduled in combination with ovarian stimulation and oocyte retrieval, such prior knowledge would benefit their female partners also, and enable couples to make more informed choices before initiating the costly process of IVF [7].

Many variables have been evaluated for their potential in predicting the success of surgical sperm retrieval via micro-TESE. These include patient age, testicular size, genetics, history of cryptorchidism or varicocele, and serum levels of follicle-stimulating hormone (FSH) and inhibin B [2]. While some of these variables can improve estimates of success rate, none is directly sensitive to spermatogenesis. The best prognostic indicator is genetic profile; men whose azoospermia results from AZFc microdeletions of the Y chromosome have a good chance of successful micro-TESE, whereas those with AZFa or AZFb microdeletions have an extremely low probability of success, and those with Klinefelter syndrome have average or favorable success rates [2]. Other variables exhibit limited predictive value, although varicocele repair has been shown to increase the chance of successful micro-TESE [2].

A recent ex vivo study of human testicular tissue specimens by Aaronson *et al.* suggested that ^{1}H-MRS may be useful in assessing spermatogenesis [8]. Using high resolution magic angle spinning spectroscopy at 11.7T, the authors observed significantly lower concentrations of phosphocholine in tissue samples exhibiting Sertoli-cell-only histology than in specimens from fertile control subjects [8]. This is consistent with phosphocholine's role as a marker of phospholipid membrane synthesis and active cell proliferation.

A small number of in vivo studies in human testes at 1.5T have corroborated these findings. Firat *et al.* reported increased choline/lipid ratios in postpubertal men compared to prepubertal boys, which they attributed to initiation of spermatogenesis [9]. Tsili *et al.* observed reductions in choline/creatine and myo-inositol/creatine ratios after age 40 in adult men, which they associated with declining spermatogenesis [10]. Parenti *et al.* found that the height of the choline peak was significantly lower in a group of patients with altered semen parameters compared to a control group with normal spermatogenesis [11].

Our goal was to investigate whether quantitative ^{1}H-MRS of the testes at 3T might provide a robust, noninvasive means of evaluating spermatogenesis in vivo. Clinical 3T scanners are widely available and offer two advantages for spectroscopy over 1.5T systems, namely increased signal-to-noise ratio (SNR) and greater frequency separation between spectral peaks. Quantitative spectroscopy can be performed by normalizing the metabolite signals to the water signal from the same voxel and correcting for the relative T1 and T2 weighting of the water and metabolite signals. This approach is preferable to taking metabolite ratios for two reasons. First, the SNR of the water exceeds that of the metabolites by four orders of magnitude. Second, in the context of spermatogenesis, water may constitute a more reliable internal reference than creatine, since the results of Aaronson *et al.* suggest differences in testicular creatine concentrations between men with normal and impaired spermatogenesis [8]. In this work we use quantitative ^{1}H-MRS at 3T to compare testicular metabolite concentrations between fertile control subjects and infertile men.

Materials and methods

Subject cohort

Nine infertile men and nine control subjects participated in the study. All provided written informed consent under a protocol approved by the local institutional review board. The mean age of the patients was 36.2 years (range 31 – 50), and each underwent a single spectroscopy exam. The control subjects made multiple visits, the longest interval between the first and last scan being 11 months; their mean age was 34.2 years (range 27 – 40) at the time of the first visit. All the controls except the youngest one had previously fathered children.

Patients were selected on the basis of their sperm count, their lack of reproductive tract obstruction, and their willingness to participate in the study. Eight had NOA and one had severe oligospermia. Genetic testing was performed in all cases. One patient had Klinefelter syndrome (47, XXY), and another had SRY-positive XX male syndrome, a very rare condition caused by translocation of the sex-determining region of the paternal Y chromosome onto the paternal X chromosome during meiotic division. The remaining patients all had normal karyotype, with no microdeletions from the Y chromosome. Five of the patients had previously undergone testicular biopsy or micro-TESE, all with negative results. The shortest interval between the surgery and the MR exam was 9 weeks. Pathology analyses were available for four patients, and in all cases revealed germ cell aplasia (also known as Sertoli-cell-only syndrome). The patient demographics and medical history are summarized in Table 1.

MR acquisition

Exams were conducted on a 3T Prisma system (Siemens Healthcare, Erlangen, Germany) using a 4-channel phased array (Siemens 'small flex' coil) for signal reception. Subjects were positioned supine on the scanner table, with a broad elasticized band wrapped around the knees to minimize motion and hold the legs together. Gauze was packed beneath the scrotum to elevate the testes close to the receive coil for improved SNR. Blankets were provided for warmth and music for relaxation.

^{1}H-MRS was performed using single-voxel point resolved spectroscopy (PRESS). In preparation for the acquisition, the B_0 field was shimmed over the spectroscopy voxel using the online Siemens 3D (image-based) and interactive (linewidth-based) shimming tools. The PRESS sequence was run with and without water suppression to allow normalization of metabolite signals to an internal water reference. Data were acquired in all subjects using an echo time (TE) of 40 ms and a repetition time (TR) of 2000 ms, with a receiver bandwidth of 1200 Hz. A 12 x 12 x 12 mm^3 voxel was prescribed in all the controls and six of the patients, with 192 averages for the water-suppressed spectrum and 4 averages for the water signal, giving acquisition times of 6:34 min and 18 sec respectively. In the remaining patients, the voxel volume was reduced, to between 10 x 6 x 6 mm^3 and 11 x 11 x 11 mm^3, to allow for the smaller size of the testes. The smallest voxel was used in the patient with Klinefelter syndrome (see Figure 1). The number of averages was doubled in these cases, resulting in an acquisition time of 12:58 min for the water-suppressed spectrum. While this more than compensated for the volume reduction in the case of an 11 x 11 x 11 mm^3 voxel, it was insufficient to preserve SNR for the smallest voxel. However, increasing the number of averages further could have been counterproductive due to the exacerbated risk of motion.

In control subjects only, the T1 and T2 times of water and metabolites were also measured by acquiring additional spectra over a range of TR and TE times as described below. Because these measurements were rather lengthy, they required separate visits. T2 values were measured in all controls and T1 values in seven controls. Since a spectrum with TE = 40ms and TR = 2000ms was included in each exam, these additional visits also provided a test of reproducibility.

T2-weighted fast spin echo (FSE) images were collected in all patients and all but one of the controls. Imaging parameters included an in-plane resolution of 0.5 x 0.5 mm^2, slice thickness of 2 mm with no gap, TE = 104 ms and TR = 4010 – 5360 ms depending on the number of slices required to cover both testes. The images were reviewed by a board-certified, fellowship-trained abdominal radiologist to assess for pathology and testicular parenchymal abnormalities, including edema, heterogeneity, and rete testis prominence. A quantitative comparison of the T2-weighted signal of the testicular parenchyma across subjects was performed by normalizing to the signal of adjacent scrotal fluid. The images were also used to calculate testicular volumes by segmenting the testes manually from surrounding tissues.

Spectral processing

Spectra were fitted using TARQUIN (version 4.3.10), a freely-available validated spectral fitting software package [12]. The basis set was chosen to be a subset of the metabolites identified by Aaronson *et al.* in testicular tissue samples [8]. Inclusion of all the metabolites reported by Aaronson *et al.* would have incurred the risk of overfitting, since many of the spectral peaks identified by magic angle spinning at ultra-high field could not be resolved in vivo. The subset was chosen by selecting only the principal peaks from the ex vivo spectra and progressively reducing the number of metabolites to the minimum required to provide a satisfactory fit to the spectra from control subjects. The final basis set (Figure 2) comprised phosphocholine (PCho), creatine (Cr), myo-inositol (mI), glutamate (Glu), glutamine (Gln), macromolecules (MM) and lipids (Lip). Since PCho cannot be resolved from choline (Cho) in vivo, the calculated concentrations of PCho should be interpreted as representing total choline (tCho). However, it should be noted that PCho has been reported to have a substantially higher concentration than Cho in testicular tissue samples [8]. Similarly phosphocreatine (PCr) cannot be resolved from Cr in vivo, so our estimated values for Cr should be interpreted as representing total creatine (tCr).

Metabolite concentrations were calculated using the unsuppressed water signal as a reference, as detailed below, assuming a testicular water content of 84% [13]. Corrections were made for the relative T1 and T2 weighting of water and metabolite signals, using the mean T1 and T2 values measured over the control subjects.

T1 measurements

T1 measurements were performed using the progressive saturation approach [14], in which several spectra are acquired over a range of TR values, providing different degrees of T1 weighting. The TR values used were 900, 1300, 2000, 4000 and 8000 ms, and the TE was kept short (40ms) to maximize SNR. T1 values were measured for metabolites and water using the PRESS sequence with and without water suppression respectively. For a TR of 2000 ms and higher, 96 averages were used for the water-suppressed acquisition and 4 averages for the water reference. For TR values of 900 ms and 1300 ms, the number of averages was increased to match the acquisition time for the run with TR=2000 ms.

The resulting spectra were processed using TARQUIN to obtain the amplitudes of the metabolite and water signals, which were then fitted as a function of TR using the following model.

$$S(\mathrm{TR}) = S_0 \left[2e^{-(\mathrm{TR}-\tau_1)/T_1} - e^{-\mathrm{TR}/T_1} - 2e^{-(\mathrm{TR}-\tau_1-\tau_2)/T_1} + 1 \right] \quad (1)$$

This model describes the partial saturation of the signal due to finite TR, and takes into account the effect of the refocusing pulses on the longitudinal magnetization through the parameters τ_1 and τ_2, where

$$\tau_1 = \frac{\mathrm{TE}_1}{2} \quad (2)$$

is the interval between the excitation pulse and the first refocusing pulse (which equals 8.3ms for the Siemens PRESS sequence) and

$$\tau_2 = \frac{\mathrm{TE}}{2} \quad (3)$$

is the interval between the first and second refocusing pulses (which equaled 20ms for our choice of TE).

Note that the model above ignores B_1^+ inhomogeneity. That is, it assumes that the excitation is a perfect 90° pulse, which nulls the longitudinal magnetization, and that the refocusing pulses are exactly 180°, thereby inverting any longitudinal magnetization that has recovered since the application of the previous radiofrequency pulse.

Note also that the procedure above produces a single T1 estimate for tCr, rather than separate T1 values for the 3.0 ppm and 3.9 ppm peaks. This is because TARQUIN assumes a fixed proton ratio between the CH_3 and CH_2 groups of Cr. Although T1 measurements at 3T in the brain suggest differences in T1 between the two peaks of Cr [14, 15], the SNR of tCr in our study did not support fitting the two peaks independently. Since T2 was calculated in an analogous manner (see below), a single T2 value is similarly reported for tCr. As a consequence, the relaxation times for tCr should be regarded as rough estimates only.

Glu and Gln had insufficient signal for T1 estimation. Consequently, T1 results are reported only for water, tCho, tCr and mI.

T2 measurements

T2 was measured by running the PRESS sequence multiple times over a range of TE values (40, 80, 160 and 250ms) using a relatively long TR (2000ms). Measurements were made for metabolites and water by repeating each acquisition with and without water suppression, using 192 and 4 averages respectively. The resulting spectra were processed using TARQUIN to obtain the amplitudes of the metabolite and water signals. To account for incomplete recovery of longitudinal magnetization between successive excitations, the raw signal amplitudes were corrected by inverting expression (1) as follows.

$$S_{\mathrm{corrected}}(\mathrm{TE}) = S(\mathrm{TE})\left[2e^{-(\mathrm{TR}-\tau_1)/T_1} - e^{-\mathrm{TR}/T_1} - 2e^{-(\mathrm{TR}-\tau_1-\mathrm{TE}/2)/T_1} + 1\right]^{-1} \quad (4)$$

This was necessary since the degree of recovery depends on TE. Note that we have substituted τ_2 = TE/2 in the above equation to make the TE-dependence explicit. For the

purposes of this correction, the T1 of water and metabolites were set to the mean values measured over the control subjects.

T2 times were calculated by fitting the logarithm of the corrected signals to a linear function of TE as follows

$$\log[S_{\text{corrected}}(\text{TE})]=\text{const}-\frac{\text{TE}}{T_2} \quad (5)$$

It was not feasible to estimate the T2 of mI because its signal dephases rapidly with TE due to strong J-coupling. As a consequence, we report T2 values only for water, tCho and tCr.

Calculation of metabolite concentrations

The spectral fitting software defines the metabolite signal as the area under the spectral peak, normalized to the number of contributing protons. With this definition, the signal S is related to the metabolite concentration C through

$$S=\eta\alpha(T_1,T_2)C \quad (6)$$

where η is a scaling factor that incorporates metabolite-independent quantities such as voxel volume and coil sensitivity, while $\alpha(T_1, T_2)$ accounts for attenuation of the signal due to relaxation processes. The attenuation can be expressed as a product of transverse relaxation and partial saturation, of which the latter is obtained from equation (1)

$$\alpha(T_1,T_2)=e^{-\text{TE}/T_2}\left[2e^{-(\text{TR}-\tau_1)/T_1}-e^{-\text{TR}/T_1}-2e^{-(\text{TR}-\tau_1-\tau_2)/T_1}+1\right] \quad (7)$$

Using water as an internal reference and noting that equation (6) applies to water as well as metabolites, we can determine the absolute metabolite concentration in units of millimolar from

$$C_m=\frac{\alpha(T_{1,w},T_{2,w})}{\alpha(T_{1,m},T_{2,m})}\frac{S_m}{S_w}C_w \quad (8)$$

where the subscripts m and w refer to metabolite and water respectively. The ratio S_m/S_w represents the metabolite signal relative to water, and is obtained directly from the spectral fitting software. The factor C_w is the water concentration in the tissue, in this case the testis. Using a literature value of 84% for testicular water content [13], and noting that the molar mass of water is 18.02 g/mol, C_w equals

$$C_w = 0.84 \frac{1000\ \mathrm{g/L}}{18.02\ \mathrm{g/mol}} = 46.6\ \mathrm{M} \quad (9)$$

The remaining factor $\alpha(T_{1,w}, T_{2,w})/\alpha(T_{1,m}, T_{2,m})$ represents the T1 and T2 weighting of the water signal relative to that of the metabolite signal. For the purposes of this correction, we used the mean T1 and T2 values for water and metabolites measured over the controls.

Statistical analysis

Nonparametric tests of significance were used throughout, since the sample sizes were too small to assume normal distributions. Within-group differences were analyzed using the Wilcoxon signed-rank test, while between-group differences were assessed using the Mann-Whitney U test. Correlations were calculated using Spearman's rank-order correlation. The threshold for statistical significance was set at p = 0.05. Reproducibility was characterized using the coefficient of variation evaluated from duplicate measurements [16].

Results

Imaging findings

No gross abnormalities were evident on the T2-weighted FSE images, although bilateral varicoceles were reported in one patient and epididymal cysts in two other patients. One patient had previously undergone orchiectomy for a Leydig cell tumor in the right testis. No evidence of edema was observed in any subject, although signal heterogeneity in the testicular parenchyma was noted in four patients. Two of these patients had previously undergone micro-TESE and the other two had not. The rete testis was prominent in four subjects, of which one was a control and three were patients. Both these features are illustrated in the lower image of Figure 6. The T2-weighted signal of the testicular parenchyma, normalized to adjacent scrotal fluid, was not significantly different between patients and controls, but had a larger standard deviation among the patients (0.567 ± 0.090 versus 0.573 ± 0.044 respectively, p=0.96).

Testicular volume was significantly lower in the patients (mean 8.4cc, range 1.3 – 27.6cc) than the controls (mean 18.4cc, range 10.8 – 27.2cc), p=0.006. The patient with the largest testes was the one with oligospermia. In the control group, the left testis was smaller than the right in all cases (mean volumes 17.5cc versus 19.3cc respectively, p=0.008). In patients, however, there was no statistically significant volume difference between left and right testes (8.9cc versus 8.7cc respectively, excluding the patient with a single testis, p=0.95).

Figure 1 shows example images from a 36-year old control subject (top) and a 33-year old patient with Klinefelter syndrome (bottom). The spatial scale is identical between the two images. Note that the patient has much smaller testes than the control, necessitating a reduction in the size of the spectroscopy voxel (arrow).

Spectral data quality

Spectra were successfully acquired in all participants, including patients with very small testes. In all controls and four patients, spectra were acquired in both testes. In the remaining patients spectra were acquired in a single testis, due to insufficient time (4 patients) or orchiectomy (1 patient). Over the control subjects, the spectral linewidth as evaluated by TARQUIN from the full width at half maximum (FWHM) of the unsuppressed water signal was 7.9 ± 1.4 Hz (mean ± standard deviation), which is equivalent to 0.064 ± 0.011 ppm. Among patients it was 13.1 ± 4.7 Hz, or 0.106 ± 0.038 ppm. The broader linewidths in the patients may be due in part to the smaller size of their testes and the correspondingly greater nonlinearity of the magnetic field variations. However, in all participants the linewidths were sufficiently narrow to resolve the peaks from Cho- and Cr-containing compounds at 3.2 ppm and 3.0 ppm respectively.

Figure 2 shows an example spectrum from the control subject of Figure 1. Overlaid is the spectral fit achieved with TARQUIN using the chosen basis set, which comprised PCho, Cr, mI, Glu, Gln, MM and Lip. The heavy black line indicates the spectral fit, while the colored curves depict the signal contributions from the various metabolites. Note that all the metabolites in this limited basis set make substantial contributions to the spectral fit, and their peaks have minimal overlap, demonstrating that the set contains little redundancy. Note also that the fit is relatively good over most of the spectral range, with the exception of a peak in the data near 3.8ppm, which is not well accounted for. This was consistent across subjects (see other examples in Figures 3, 4 and 6).

Data acquired with TE = 40ms and TR = 2000ms in the control subjects over multiple visits were used to estimate reproducibility. The coefficients of variation for the metabolite signals relative to water were 11% for tCho, 19% for tCr and 19% for mI.

T1 and T2 results

Figure 3 shows an example of a dataset used to calculate metabolite T1 values. On the left is a series of spectra acquired from a 41-year old control subject at different TR periods. Note that the peaks corresponding to tCho, tCr and mI grow as TR increases, while the signal from lipids remains relatively constant. This reflects the fact that the T1 of lipids is short compared to the TR values used in this study, while the T1 times of the other metabolites are not. On the lower right of the figure are graphs of the signals from water, tCho and tCr as determined by TARQUIN. The signals are plotted as a function of TR, together with best-fit curves to the saturation recovery model given in equation (1). Note that the model provides an excellent fit to the water signal. This was observed consistently across subjects, thereby justifying the omission of B_1^+ inhomogeneity effects from the model.

Figure 4 shows an example of a dataset used to calculate metabolite T2 times. On the left are a series of spectra acquired from a 33-year old control subject at different TE values. Note that as TE increases the baseline flattens and the spectrum simplifies, leaving the tCho and tCr peaks as the dominant features. These peaks nevertheless diminish in height with TE due to T2 relaxation. Note also that the relative phase of the mI peaks varies with TE due to J-coupling. This dephasing precluded measurement of T2 for mI. On the lower right are

graphs of the signals from water, tCho and tCr as determined by TARQUIN. The signals are plotted as a function of TE on a semilogarithmic scale, together with the lines of best fit as described by equation (5). Note that the logarithm of the water signal is very well fitted by a linear function of TE. However, the tCho signal and, to a lesser extent, the tCr signal show substantial deviations from the model; in particular, at TE = 80ms the tCho signal falls below the line of best fit, while at TE = 160ms it lies above. This trend was observed in a majority of subjects, and may reflect shortcomings of the spectral fitting procedure.

T1 and T2 results over the control subjects are presented in Figure 5 and summarized in Table 2. Note that the range and standard deviation for tCr are higher than for the other metabolites, reflecting the lower SNR of tCr and the correspondingly greater scatter among its measured relaxation times. The T2 values for tCho should be interpreted with caution given the relatively poor quality of the fits.

Metabolite concentrations in patients and controls

Figure 6 compares spectra from a 35-year old fertile control subject (top) and a 33-year old azoospermic patient with germ cell aplasia (bottom). Note that the tCho concentration is dramatically reduced in the patient compared to the control, and the patient's tCr and mI concentrations are both below the level of detectability.

Figure 7 compares tCho, tCr and mI concentrations between patients and controls. For each individual, metabolite concentrations were estimated by averaging over all spectra acquired at TE = 40ms and TR = 2000ms, i.e. over left and right testes where data were available, and over multiple visits in the case of the controls. The concentrations of tCho and tCr are expressed in absolute units of millimolar [mM]. In the case of mI, T2 could not be measured reliably due to strong J-coupling and the results are displayed in terms of the signal relative to water. Note, however, that if T1 and T2 corrections had been made for mI in the same manner as for tCho and tCr, the results would simply have been scaled uniformly; the relative values and statistics would be unchanged.

As demonstrated by the plots, tCho, tCr and mI concentrations were all significantly lower in patients than controls. In particular, tCho and mI exhibit no overlap of values between groups. The patient with the highest levels of tCho was the 50-year old man with oligospermia. Since this subject could be considered an outlier, both in terms of his age and because his condition was less severe than that of the other patients, statistical measures were calculated both including and excluding him from the patient group. These are summarized in Table 3.

Metabolite concentrations showed no statistically significant correlation with testis volume either for the control group alone or for the patient group alone. Over the entire cohort, however, including both patients and controls, testis volume was positively correlated with all the measured metabolites ($\rho = 0.71$, $p = 0.002$ for tCho, $\rho = 0.65$, $p = 0.005$ for tCr and $\rho = 0.69$, $p = 0.002$ for mI, where ρ is Spearman's rank-order correlation coefficient). This reflects the fact that both testis volume and metabolite concentrations were lower in patients than controls.

Discussion

The most prominent peak in the spectra from control subjects was that of choline-containing compounds, which are involved in phospholipid synthesis and degradation, and thus constitute a marker of membrane turnover and active cell proliferation. Their high concentration in controls reflects the rapid rate of spermatogenesis in normal testes (about 4 million spermatozoa per gram of testicular tissue per day [17]). Averaged over our control group, tCho concentration was 4.4 mM, which is in rough agreement with the value of 3.6 mM (representing the sum of Cho and PCho concentrations) reported by Aaronson *et al.* [8] from specimens of normal testicular tissue. We observed significantly lower tCho concentrations in patients than controls, with no overlap in values between groups. This also is consistent with the observations of Aaronson *et al.* and suggests that tCho as measured by ^{1}H-MRS may be valuable as a noninvasive biomarker of spermatogenesis.

Other metabolites identified in the spectra of our control subjects were tCr, mI, Glu, Gln, macromolecules and lipids. Total creatine (representing the sum of Cr and PCr) plays a crucial role in cellular energy metabolism through the creatine kinase reaction, in which ADP is phosphorylated by PCr to produce ATP and Cr. In cells such as spermatozoa that consume energy rapidly, PCr serves as an energy reservoir for rapid regeneration of ATP and intracellular energy transport via the PCr shuttle. We observed significantly lower tCr concentrations in patients than controls. Aaronson *et al.* reported a similar trend [8], although the between-group differences in their study did not reach statistical significance. These findings suggest that the common practice of using tCr as an endogenous concentration reference may not be appropriate in studies of spermatogenesis.

Myo-inositol is a cyclic sugar alcohol that is important in sperm motility [18, 19]. Its synthesis involves two enzymes, myo-inositol-1-phosphate synthase and myo-inositol monophosphatase-1, which are produced in the germinal and Sertoli cells of the seminiferous epithelium [20]. We observed significantly lower mI concentrations in patients than controls, consistent with the fact that all our patients with known pathology had germ cell aplasia. Aaronson *et al.* reported a similar trend in mI values [8], but without statistical significance.

The study had a number of limitations. The testicular water content used in the calculation of metabolite concentrations was assumed to be constant across individuals and equal to the literature value [13]. Any adjustment in this value would simply scale the metabolite concentrations uniformly for all subjects and not alter the statistics. However, any differences in water content among subjects would affect our estimation of their relative metabolite concentrations.

The T1 and T2 values used in the estimation of metabolite concentrations were also assumed to be constant across individuals, and equal to the mean values measured in the control subjects. While any differences in T1 and T2 among subjects could in principle affect our estimates of their relative metabolite concentrations, the impact would be small because the spectra used to calculate metabolite concentrations were acquired with relatively long TR (2000ms) and short TE (40ms), and were thus only weakly T1 and T2 weighted. Note that,

since T1 and T2 measurements are inherently noisy, our use of mean T1 and T2 values rather than subject-specific values avoids the introduction of scatter into the final concentration estimates.

A related limitation concerns the accuracy of our metabolite T2 measurements. In a majority of control subjects, the metabolite signals showed consistent deviations from monoexponential decay when plotted as a function of TE. This trend was particularly pronounced for tCho, but was also evident for tCr, and may be due to the proximity of their peaks to those of mI, which change phase with TE due to strong J-coupling. Any error in the fitting of mI could skew the baseline, which would in turn bias the estimates of the tCho and tCr signals in a TE-dependent manner.

A further limitation of the study concerns the heterogeneity of the patient and control cohorts. The patient group was necessarily heterogeneous since it included individuals with rare conditions. The control group may have been somewhat heterogeneous also, since we did not require semen analysis of our control subjects, but rather accepted their statements of prior paternity as evidence of fertility. The youngest man in the control group had not yet started a family, so in his case we had no evidence of fertility. However, his tCho and tCr concentrations were well within the range of the other controls, and his mI concentration, while lower than that of the other controls, was only marginally so.

In conclusion, using quantitative ^{1}H-MRS of the testes at 3T, we observed lower concentrations of tCho, tCr and mI in infertile patients than in fertile controls. These metabolites may be valuable as noninvasive biomarkers of spermatogenesis. While the technique will require further validation and refinement in a larger cohort, it may have applications in the clinical management of patients with azoospermia. In particular, if it can be shown that MRS successfully predicts the absence or presence of sperm in patients scheduled for micro-TESE, it would provide a means to determine noninvasively which patients are optimal candidates for surgical sperm retrieval before a couple embarks on IVF.

Acknowledgments

Source of Funding: This work was supported by the Departments of Radiology and Urology of the New York University School of Medicine, by Siemens Healthcare and by the National Institutes of Health under grant P41 EB017183.

References

1. Cocuzza M, Alvarenga C, Pagani R. The epidemiology and etiology of azoospermia. Clinics (Sao Paulo). 2013; 68(Suppl 1):15–26. [PubMed: 23503951]
2. Bernie AM, Ramasamy R, Schlegel PN. Predictive factors of successful microdissection testicular sperm extraction. Basic Clin Androl. 2013; 23:5. [PubMed: 25763186]
3. Schlegel PN. Testicular sperm extraction: microdissection improves sperm yield with minimal tissue excision. Hum Reprod. 1999; 14(1):131–5. [PubMed: 10374109]
4. Tsujimura A. Microdissection testicular sperm extraction: prediction, outcome, and complications. Int J Urol. 2007; 14(10):883–9. [PubMed: 17880285]
5. Ramasamy R, Yagan N, Schlegel PN. Structural and functional changes to the testis after conventional versus microdissection testicular sperm extraction. Urology. 2005; 65(6):1190–4. [PubMed: 15922422]

6. Takada S, Tsujimura A, Ueda T, et al. Androgen decline in patients with nonobstructive azoospemia after microdissection testicular sperm extraction. Urology. 2008; 72(1):114–8. [PubMed: 18372017]
7. Chambers GM, Sullivan EA, Ishihara O, et al. The economic impact of assisted reproductive technology: a review of selected developed countries. Fertil Steril. 2009; 91(6):2281–94. [PubMed: 19481642]
8. Aaronson DS, Iman R, Walsh TJ, et al. A novel application of 1H magnetic resonance spectroscopy: non-invasive identification of spermatogenesis in men with non-obstructive azoospermia. Hum Reprod. 2010; 25(4):847–52. [PubMed: 20124393]
9. Firat AK, Ugras M, Karakas HM, et al. 1H magnetic resonance spectroscopy of the normal testis: preliminary findings. Magn Reson Imaging. 2008; 26(2):215–20. [PubMed: 17728090]
10. Tsili AC, Astrakas LG, Ntorkou A, et al. MR Spectra of Normal Adult Testes and Variations with Age: Preliminary Observations. Eur Radiol. 2016; 26(7):2261–7. [PubMed: 26474986]
11. Parenti GC, Albarello F, Campioni P. Role of MR Spectroscopy (H1-MRS) of the Testis in Men with Semen Analysis Altered. Reprod Syst Sex Disord. 2016; 5(3):182.
12. Wilson M, Reynolds G, Kauppinen RA, et al. A constrained least-squares approach to the automated quantitation of in vivo (1)H magnetic resonance spectroscopy data. Magn Reson Med. 2011; 65(1):1–12. [PubMed: 20878762]
13. Altman PL, Dittmer DS. Biology Data Book. 1964:1–631. Amrl-Tr-64-100. AMRL TR.
14. Traber F, Block W, Lamerichs R, et al. 1H metabolite relaxation times at 3.0 tesla: Measurements of T1 and T2 values in normal brain and determination of regional differences in transverse relaxation. J Magn Reson Imaging. 2004; 19(5):537–45. [PubMed: 15112302]
15. Mlynarik V, Gruber S, Moser E. Proton T (1) and T (2) relaxation times of human brain metabolites at 3 Tesla. NMR Biomed. 2001; 14(5):325–31. [PubMed: 11477653]
16. Hyslop NP, White WH. Estimating precision using duplicate measurements. J Air Waste Manag Assoc. 2009; 59(9):1032–9. [PubMed: 19785269]
17. Amann RP, Howards SS. Daily spermatozoal production and epididymal spermatozoal reserves of the human male. J Urol. 1980; 124(2):211–5. [PubMed: 6772801]
18. Bahat A, Eisenbach M. Human sperm thermotaxis is mediated by phospholipase C and inositol trisphosphate receptor Ca2+ channel. Biol Reprod. 2010; 82(3):606–16. [PubMed: 19955332]
19. Condorelli RA, La Vignera S, Bellanca S, et al. Myoinositol: does it improve sperm mitochondrial function and sperm motility? Urology. 2012; 79(6):1290–5. [PubMed: 22656408]
20. Chauvin TR, Griswold MD. Characterization of the expression and regulation of genes necessary for myo-inositol biosynthesis and transport in the seminiferous epithelium. Biol Reprod. 2004; 70(3):744–51. [PubMed: 14613899]

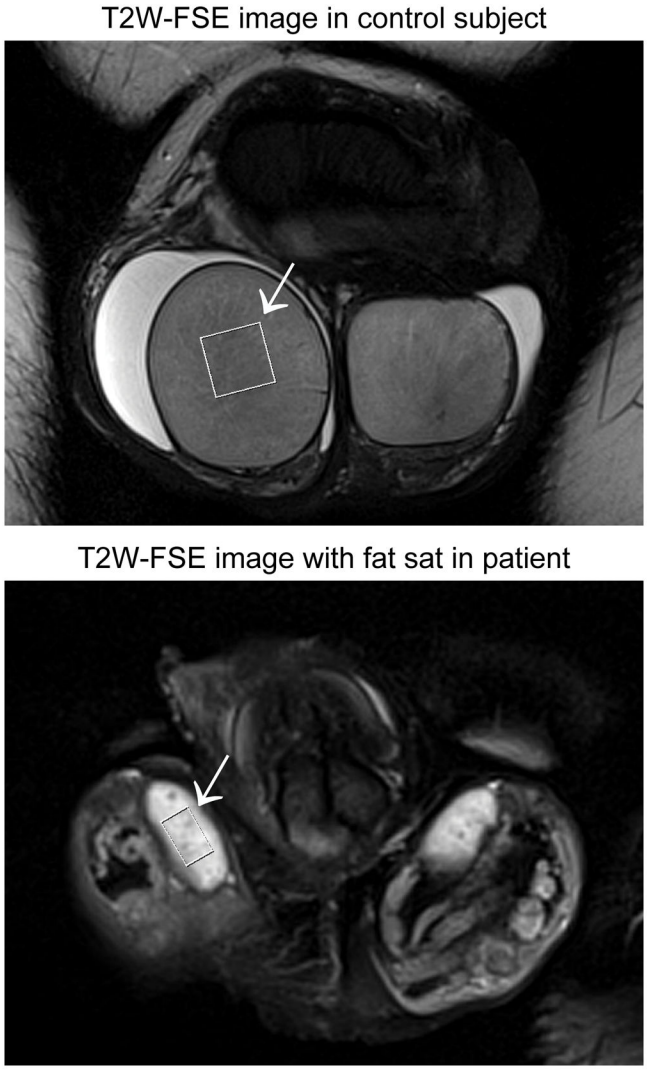

Figure 1.

Coronal T2-weighted fast spin echo (FSE) images acquired in a 36-year old control subject (top) and a 33-year old patient with Klinefelter syndrome (bottom). The image from the patient was acquired with fat saturation to improve conspicuity of the testes. The spatial scale is matched between the two images to facilitate comparison of testicular size between the control subject and the patient. Averaged over left and right, testicular volume is 19.5 cc in the control subject and 1.5 cc in the patient. The arrow in each case indicates the PRESS box over which single-voxel spectra were acquired. It measures 12 x 12 x 12 mm^3 in the control subject, but was reduced to 10 x 6 x 6 mm^3 in the patient to fit within the margins of the testis.

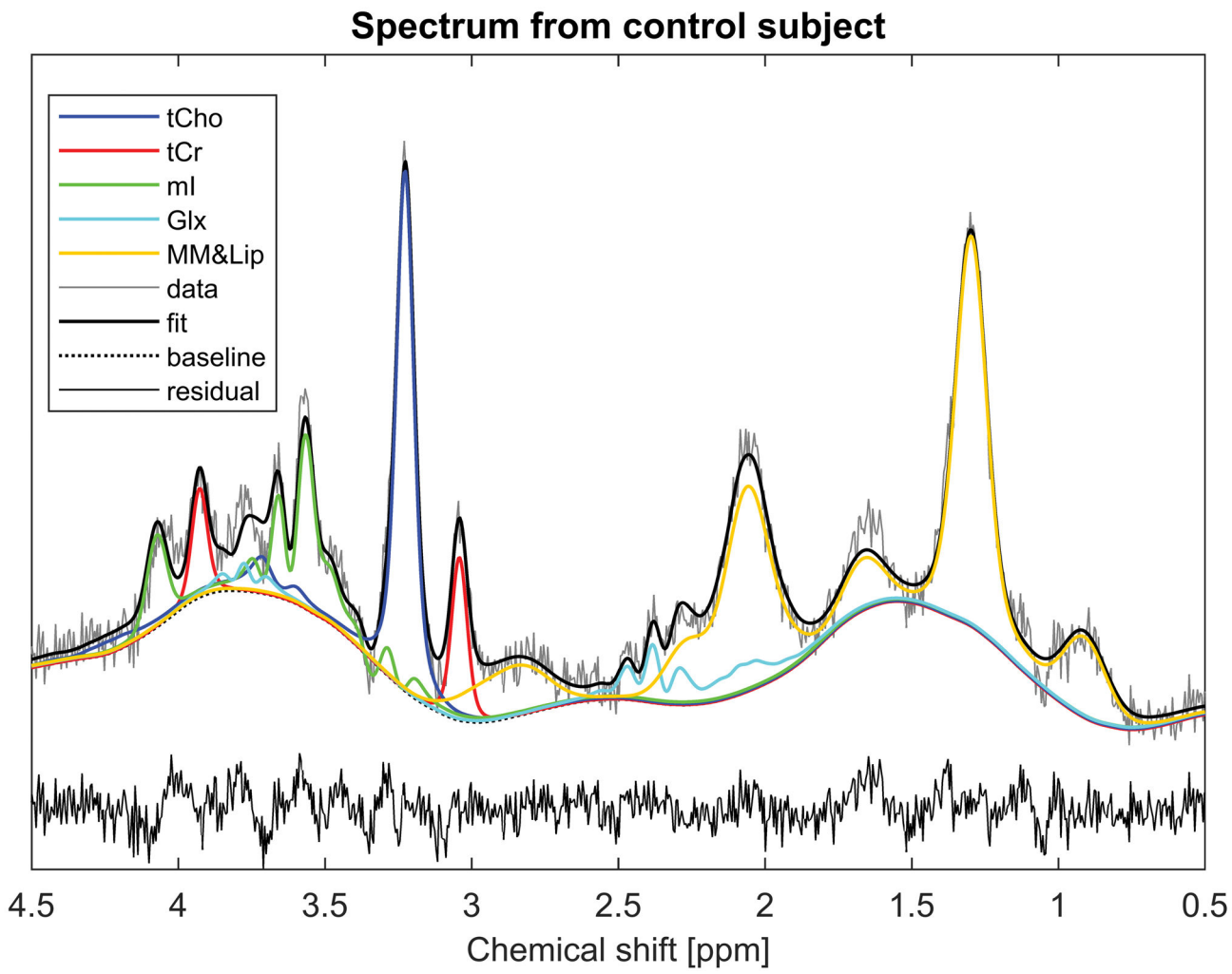

Figure 2.

A single-voxel spectrum from the 36-year old control subject shown in Figure 1. The spectrum was acquired with TE = 40ms and TR = 2000 ms, and fitted using TARQUIN [12]. Individual curves show the contributions from the various metabolites in the basis set. Abbreviations are as follows: tCho = total choline, tCr = total creatine, mI = myo-inositol, Glx = glutamate and glutamine, MM&Lip = macromolecules and lipids.

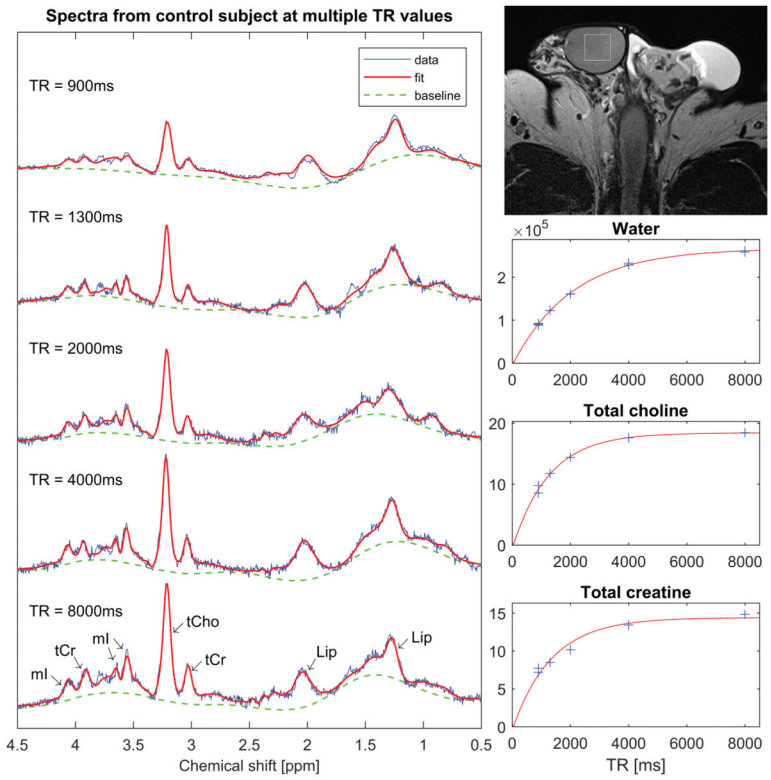

Figure 3.

Single-voxel spectra from a 41-year old control subject. The spectra were acquired with TE = 40ms and multiple TR values for estimation of metabolite T1 times. The vertical and horizontal scales are identical across all spectra to facilitate comparison of the signal amplitudes at different TR values. On the top right is an axial T2-weighted FSE image showing placement of the spectroscopy voxel. Below the image are graphs showing fits of the water and metabolite signals as a function of TR to saturation-recovery curves.

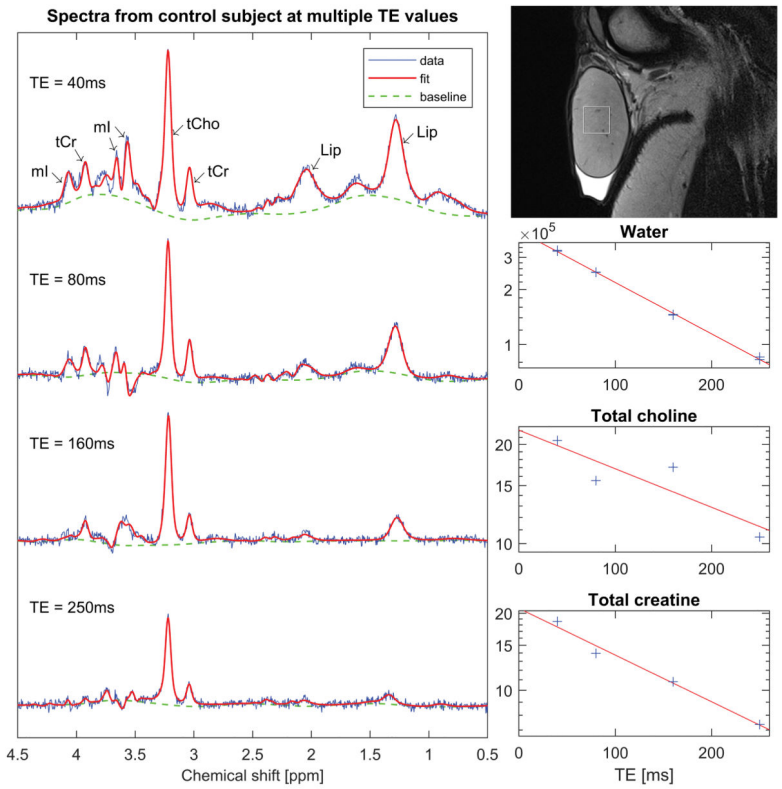

Figure 4.

Single-voxel spectra from a 33-year old control subject. The spectra were acquired with TR = 2000ms and multiple TE values for estimation of metabolite T2 times. The vertical and horizontal scales are identical across all spectra to facilitate comparison of the signal amplitudes at different TE values. On the top right is a sagittal T2-weighted FSE image showing placement of the spectroscopy voxel. Below the image are graphs showing the water and metabolite signals as a function of TE on a semilogarithmic scale, together with the lines of best fit.

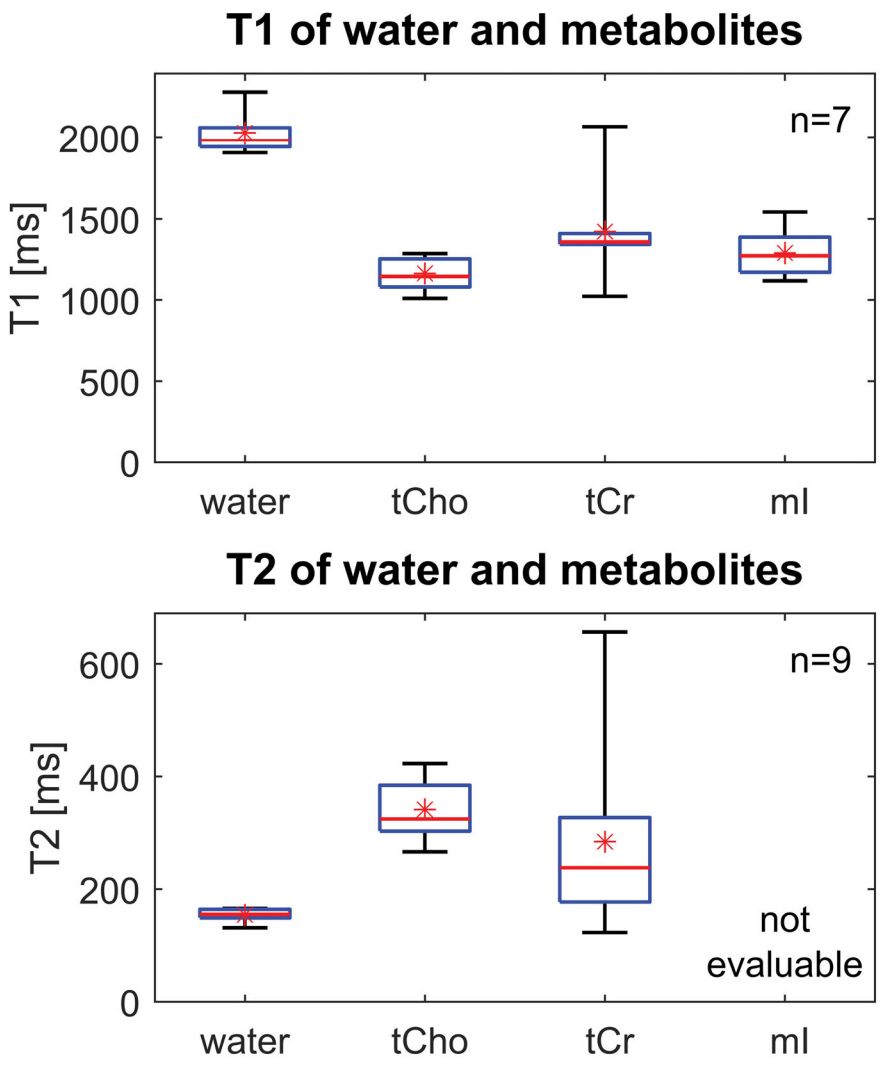

Figure 5.

Box-and-whisker plots showing T1 and T2 values for water and metabolites measured over the control subjects. Medians are displayed using a horizontal line, while means are indicated with an asterisk. The T2 of mI could not be measured reliably due to strong J-coupling. The large range of values for tCr reflects its low SNR, which produces more scatter in its T1 and T2 measurements.

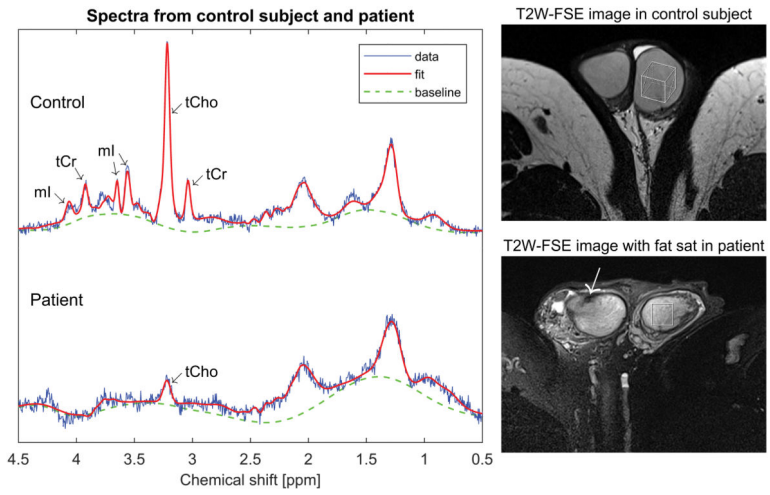

Figure 6.

Single-voxel spectra from a 35-year old control subject (top) and a 33-year old azoospermic patient with germ cell aplasia (bottom). The vertical scale is normalized to the water signal in both cases. Note that the patient has a much smaller tCho peak than the control subject and no discernable tCr or mI peaks. To the right are axial T2-weighted FSE images from the control subject (top) and the patient (bottom) showing the locations of the spectroscopy voxel. The patient image was acquired with fat saturation, and demonstrates a prominent rete testis (arrow) and some signal heterogeneity in the testicular parenchyma.

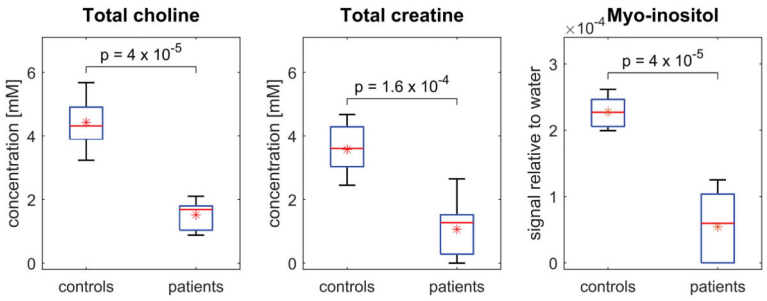

Figure 7.

Box-and-whisker plots comparing tCho, tCr and mI concentrations between all patients and controls. Medians are displayed using a horizontal line, while means are indicated with an asterisk. Note that patients exhibit significantly lower concentrations of all metabolites than control subjects. In particular, tCho and mI concentrations show no overlap of values between groups. Metabolite signals were normalized in each case to the unsuppressed water signal. Corrections for T1 and T2 weighting were performed for tCho and tCr, allowing the concentrations to be expressed in absolute units of millimolar [mM]. For mI, T2 could not be measured reliably due to strong J-coupling, and the results are displayed as signal relative to water.

Table 1

Patient demographics and clinical history

Age	Diagnosis	FSH	Chromosomal abnormalities	Clinical history
31	NOA	17	none	Negative bilateral micro-TESE 2 years prior to MR exam; pathology analysis revealed germ cell aplasia
40	NOA	23	none	No surgery
50	severe oligospermia	7	none	Sperm count of 1000 after varicocele repair. No biopsy or sperm extraction surgery.
35	NOA	19	none	Negative bilateral micro-TESE at outside institution 3 years prior to MR exam; subsequent varicocele repair
32	NOA	30	none	Negative bilateral micro-TESE 9 weeks prior to MR exam; pathology analysis revealed germ cell aplasia
33	NOA	20	none	Negative bilateral micro-TESE 14 weeks prior to MR exam; pathology analysis revealed germ cell aplasia
34	NOA	25	none	Negative biopsy at outside institution 2 years prior to MR exam; pathology unknown
33	NOA	27	47, XXY (Klinefelter)	No surgery
38	NOA	49	46, SRY-positive XX	Orchiectomy for Leydig cell tumor; surrounding tissue exhibited germ cell aplasia. No surgery on remaining testis.

FSH = follicle-stimulating hormone; NOA = non-obstructive azoospermia; micro-TESE = microdissection testicular sperm extraction; SRY = sex-determining region of the Y chromosome

Table 2

T1 and T2 values (mean ± standard deviation) measured over control subjects

Relaxation time	Water	Total choline	Total creatine	Myo-inositol	n
T1 [ms]	2028 ± 125	1164 ± 105	1421 ± 314	1291 ± 150	7
T2 [ms]	154 ± 11	342 ± 53	285 ± 167	Not evaluable	9

Table 3

Mean (and range) of metabolite signals relative to water and absolute metabolite concentrations in patients and controls

	Total choline		Total creatine		Myo-inositol	n
	Signal relative to water (x 10^4)	Concentration [mM]	Signal relative to water (x 10^4)	Concentration [mM]	Signal relative to water (x 10^4)	
controls	1.44 (1.05 – 1.84)	4.4 (3.2 – 5.7)	1.04 (0.71 – 1.36)	3.6 (2.5 – 4.7)	2.28 (1.99 – 2.62)	9
patients	0.49 (0.29 – 0.68)	1.5 (0.9 – 2.1)	0.31 (0.00 – 0.77)	1.1 (0.0 – 2.7)	0.54 (0.00 – 1.25)	9
	0.47 (0.29 – 0.59) *	1.4 (0.9 – 1.8) *	0.29 (0.00 – 0.77) *	1.0 (0.0 – 2.7) *	0.53 (0.00 – 1.25) *	8 *
p-value	4×10^{-5}		1.6×10^{-4}		4×10^{-5}	
	8×10^{-5} *		3×10^{-4} *		8×10^{-5} *	

* Excluding the 50-year old patient with oligospermia